ACS APPLIED MATERIALS & INTERFACES

Research Article

Cite This: ACS Appl. Mater. Interfaces 2019, 11, 41821−41827

www.acsami.org

Effect of Lateral Size and Surface Passivation on the Near-Band-Edge Excitonic Emission from Quasi-Two-Dimensional CdSe Nanoplatelets

Jiahao Yu,[†,‡] Chaojian Zhang,[†] Guotao Pang,[†] Xiao Wei Sun,[†] and Rui Chen*[,†]

[†]Department of Electrical and Electronic Engineering, Southern University of Science and Technology, Shenzhen, Guangdong 518055, P. R. China

[‡]Harbin Institute of Technology, Harbin 150001, P. R. China

Supporting Information

ABSTRACT: As a new type of quasi-two-dimensional nanomaterial, CdSe nanoplatelets (NPLs) possess excellent properties such as narrow emission peak, large absorption cross section, and a low threshold of amplified spontaneous emission. However, the origin of emission especially at low temperatures has not been studied clearly up till now. Here, we study the temperature-dependent photoluminescence of CdSe NPLs which show two emission peaks at low temperatures. It is interesting to note that the intensity of the low-energy peak shows a correlation with laser irradiation time. Moreover, the low-temperature PL spectra of four CdSe NPLs with different lateral sizes demonstrate the relationship of low-energy peaks with the surface. It has been confirmed that CdSe NPLs with larger surface areas to volume ratio have stronger low-energy emissions, which is ascribed to the surface-state-related emission. Finally, surface passivation of CdSe NPLs attenuates the intensity of the low-energy peak, which further verifies our model. Our results demonstrate the critical significance of surface in CdSe NPLs for their optical properties, which is crucial for the application of optoelectronic devices.

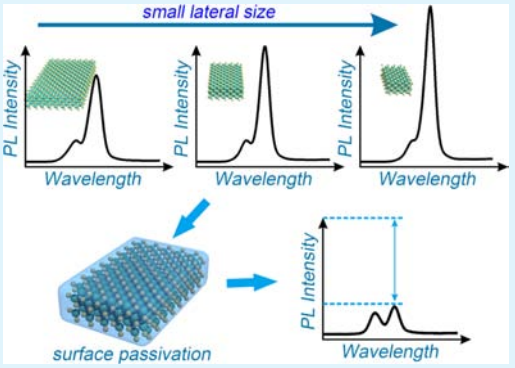

KEYWORDS: *CdSe nanoplatelets, two-dimensional nanomaterials, optical property, surface state, surface passivation.*

INTRODUCTION

When the size of the semiconductor reduces to the nanoscale, many unique physical properties are induced by the quantum confinement effects, which is important for fundamental physics investigation and new optoelectronic devices application. At present, the preparation of such nanoscale semiconductor materials mainly includes epitaxial growth and chemical solution method. Compared with the epitaxial growth, the chemical colloidal method has the advantages of low cost, good dispersibility, accurate size, and shape adjustment. Since the synthesis of colloidal semiconductor quantum dots (QDs) realized in 1993,[1] this nanometer-sized material has received intensive attention in scientific research. Due to high luminous efficiency and adjustable emission wavelength, colloidal QD materials have been widely investigated for light-emitting diodes,[2−4] biosensors,[5,6] and lasers.[7−9] CdSe is one of the most well-known II−VI semiconductor QDs. For quite a long time, changing the size and composition of this spherical nanocrystal for improved optical performance has been the main direction of research. With further development of synthetic technology, one-dimensional strip-shaped nanostructures and derived complex structures, including CdSe nanorods and tetrapod-shaped structures,[10−15] have gradually emerged. The shape change of material induced some unique optical properties compared to zero-dimensional QDs. In recent years, a new type of quasi-two-dimensional nanostructure has been synthesized which attracted intensive attention.[16−24] These planar-shaped nanocrystals are commonly referred to as nanoplatelets (NPLs). The CdSe NPLs typically are only a few monolayers (MLs) in thickness. And therefore, a very strong quantum confinement effect exists in the vertical direction compared to the larger lateral dimensions. Ascribed to the precise control of the thickness, CdSe NPLs have a very narrow emission. Generally, the emission width of CdSe NPLs is around 10 nm, which is one-third of the traditional CdSe QDs.[18,25] In addition, CdSe NPLs have been found to have a large absorption cross section, a faster radiation recombination rate, and ultralow threshold of amplified spontaneous emission.[25−29] These properties make CdSe NPLs a promising optical material for light-emitting diodes and lasers.[30−32]

However, up till now, the optical property of CdSe NPLs, such as the emission mechanism, is still under debate, which has hindered further development of device applications. In recent years, it has been reported that CdSe NPLs have two close emissions at cryogenic temperature.[33−37] Here, the two

Received: September 5, 2019
Accepted: October 15, 2019
Published: October 15, 2019

DOI: 10.1021/acsami.9b16044
ACS Appl. Mater. Interfaces 2019, 11, 41821−41827

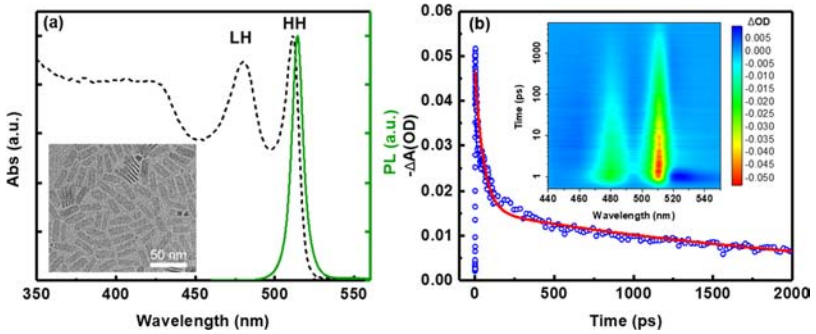

Figure 1. (a) Emission and absorption spectra of 4 MLs CdSe nanoplatelets. Inset: transmission electron microscopy image of CdSe NPLs. (b) The bleach kinetic of electron-heavy hole exciton. The red line is the fitted curve. The inset shows the transient absorption (TA) spectra of 4 MLs CdSe NPLs.

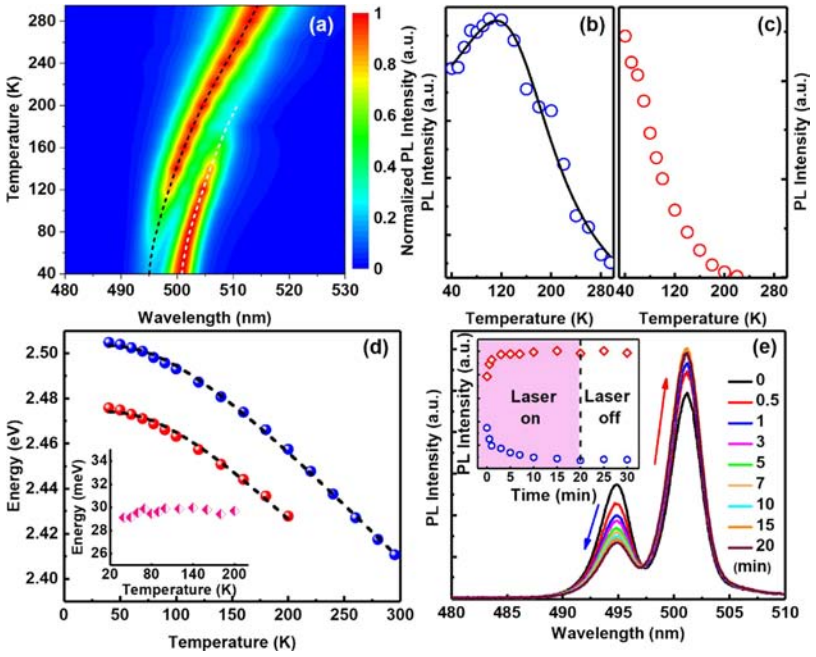

Figure 2. (a) Temperature-dependent mapping of the PL spectrum with white and black dashed lines show the trend of the peak positions. (b, c) The PL intensity of the high-energy peak and the low-energy peak as a function of temperature, respectively. (d) The temperature-dependent peak energy of the two peaks and the fitted curve (black dash line). The inset shows the energy difference between the two peaks with changing temperature. (e) The emission spectra with different irradiation times at 30 K. The inset shows the intensity of two peaks as a function of irradiation time.

emission peaks are referred to as high-energy peak and low-energy peak, respectively. Until now, the origin of these two peaks is still not clear. In the previous investigations, most of the results agree that the high-energy peak is free exciton emission. However, there are many different explanations for the origin of the low-energy peak. Early discussion proposes that the low-energy peak originated from phonon line emission, which has been enhanced due to the self-stacking of CdSe NPLs.[33,34] In later work, the two emissions were assigned to s- and p-type ground and excited state emission.[35] While in recent studies, the origin of the low-energy peak was related to charged excitons or excimer-like state emission of stacked CdSe NPLs.[36,37] The emission mechanism of the low-energy peak at low temperatures may affect the optical properties of CdSe NPLs at room temperature, so it is critical to have a clear understanding of the origin of the low-energy peak.

In this article, based on systematic laser spectroscopy, it has been observed that the low-energy emission from CdSe NPLs was closely related to the surface states (SS). It is found during the experiment that the intensity of the low-energy peak will be influenced by laser illumination at low temperatures. In addition, by comparing NPLs with different lateral sizes, it is found that the intensity of the low-energy peak shows a correlation with the lateral area. Based on investigations, it is concluded that the low-energy peak was a surface-state-related emission, which is finally verified by surface passivation. Our results reveal the effect of surface on the optical properties of two-dimensional CdSe NPLs, which is important for further optoelectronic device applications.

RESULTS AND DISCUSSION

Figure 1a shows the absorption and photoluminescence (PL) spectra of CdSe NPLs at room temperature. The absorption spectra (black dash line) shows two clear excitonic absorption peaks, which can be ascribed to the quasi-two-dimensional structure of CdSe NPLs. The two absorption peaks correspond

DOI: 10.1021/acsami.9b16044
ACS Appl. Mater. Interfaces 2019, 11, 41821−41827

to the electron-light hole (480 nm) and the electron-heavy hole (511 nm) transition, respectively.[18] The PL spectra (green solid line) show a very sharp emission peak and small Stokes shift. Since the CdSe NPLs are only a few nanometers in thickness, much smaller than the lateral sizes, NPLs have a very strong thickness-dependent quantum confinement effect. Based on the emission wavelength located at 514 nm, the thickness of the CdSe NPLs discussed herein can be determined to be 4 MLs.[18,19] The full width at half-maximum is about 39 meV, which implies good uniformity of the CdSe NPLs' thickness. The inset of Figure 1a shows the transmission electron microscopy image (TEM) of 4 MLs CdSe NPLs, which have an approximately rectangular shape with uniform size distribution. The length of this CdSe NPLs is about 25 nm and the width is around 8 nm. The inset of Figure 1b shows the femtosecond pump-probe transient absorption spectra of CdSe NPLs. Two clear exciton bleach signals appear after the pump light reaches the sample, which were generated due to the electron state filling at the conduction band edge. The two exciton bleach signals located at 480 and 511 nm can be attributed to electron to light-hole and heavy-hole transition, respectively, which is consistent with the absorption spectrum discussed above. The bleach kinetic of electron-heavy hole exciton is shown in Figure 1b. It can be found that there is a very fast decay path followed by a slow decay path. Considering the high power density of laser excitation during the measurement, the rapid process is considered to be a multiexciton collision and recombination process.[38] The slower process is the recombination of single excitons with a fitted lifetime of about 2.5 ns. This lifetime is consistent with the reported results and is much faster than the CdSe QDs.[18] All of the above results demonstrate that the prepared CdSe NPLs have 4 MLs two-dimension plane structure and good size uniformity.

To investigate the optical property of CdSe NPLs at low temperatures, the temperature-dependent PL measurement was conducted. Figure 2a shows the mapping of the temperature-dependent PL spectrum with normalized intensity, where the white and black dash lines indicate the tendency of the peak positions with temperature. It can be clearly seen that there are two emission peaks at low temperatures. At 40 K, the low-energy peak dominates the entire emission spectrum. However, with the increase of temperature, the intensity of the low-energy peak gradually decreases, and finally, only the high-energy peak remains at room temperature. Figure 2b,c shows the normalized PL intensity of the high-energy peak (blue circle) and the low-energy peak (red circle) as a function of temperature. It can be seen that the intensity of the high-energy peak shows a slight increase first and then gradually decreases with increasing temperature, while the intensity of the low-energy peak continues to decrease and disappears substantially at 220 K. This reason of the phenomenon will be discussed later. The PL peak position of the high-energy peak (blue dot) and the low-energy peak (red dot) of the CdSe NPLs as a function of temperature is shown in Figure 2d. The high-energy peak blue-shifted about 94 meV when the temperature decreased from room temperature to 40 K. The low-energy peak appears at 220 K and has the same trend as the high-energy peak. The energy difference between the two peak positions at different temperatures is a constant value (29 meV), as shown in the inset of Figure 2d. The energy shift of the high-energy peak can be well-fitted with the following expression proposed by O'Donnell and Chen[39]

$$E_g(T) = E_g(0) - \frac{2SE_{LO}}{\exp(E_{LO}/k_BT) - 1} \quad (1)$$

where $E_g(0)$ is the band gap of the material at 0 K, S is the Huang-Rhys factor, E_{LO} is the average phonon energy, and k_B is the Boltzmann constant. It can be extracted from the fitting result that E_{LO} = 24.7 meV and S = 3.08. These values are in good agreement with the result in the papers for CdSe bulk materials and QDs.[40−42] Therefore, the high-energy peak can be confirmed to be the free exciton emission.

Next, temperature-dependent free exciton emission will be discussed. It is common for a semiconductor that the PL intensity will gradually decrease with increasing temperature, due to the thermal escape of carriers or the thermal activation of nonradiative recombination centers. However, the free exciton emission of CdSe NPLs shows a slight increase when the temperature increases from 40 to 120 K. The increase in the PL intensity implies that more carriers recombine radiatively near the band edge. In the absence of external carriers, this observation can only be related to the release of carriers in the localized state (LS) due to the increased temperature. Here, a modified Arrhenius equation is used to fit the temperature-dependent PL intensity of free exciton emission

$$I(T) = I_0 \frac{1 + A\exp(-E_a/k_BT)}{1 + B\exp(-E_b/k_BT)} \quad (2)$$

where E_a is the bonding energy of localized state, E_b is the activation energy, and A and B are constants. The value of E_a and E_b obtained from the fitting were 10.5 and 75 meV, respectively. CdSe NPLs have greater activation energy than other CdSe materials,[43] which is consistent with their larger exciton binding energy.

It is interesting to note that the intensity of the near-band-edge emission can be greatly influenced by laser irradiation, as shown in Figure 2e. The temperature of the sample is kept at 30 K. With the increase of the laser irradiation time, the intensity of the free exciton emission gradually decreases, while the intensity of the low-energy peak increases. After 15 min, the intensity of the two peaks tends to be stable. It should be noticed that the position of these two peaks maintains the same, which implies that the change of intensity is not related to the thermal effect induced by the laser excitation. In addition, after the laser was turned off for 10 min, the intensity of the two peaks did not recover but remained substantially unchanged, as shown in the inset of Figure 2e. Therefore, laser irradiation brings an irreversible effect to the emission of CdSe NPLs. Early literature suggested that the low-energy peak is a phonon line recombination.[33,34] However, laser irradiation should not influence the intensity of the phonon line. More importantly, the energy difference between the two emissions from our samples (29 meV) is also not the same as the longitudinal optical phonon energy of CdSe materials (25 meV). Therefore, this interpretation can be ruled out. Similarly, the recently proposed excimer-like state emission of stacked CdSe NPLs cannot explain this phenomenon. Considering that the CdSe NPLs have a large surface area, we thought that the low-energy peak may originate from surface-related states. Laser irradiation induces an increase of surface states which saturate after a period of time, thus causing an increase in the intensity of the low-energy peak.

To further verify our hypothesis, CdSe NPLs with different lateral sizes were prepared and discussed. The lateral area of

DOI: 10.1021/acsami.9b16044
ACS Appl. Mater. Interfaces 2019, 11, 41821−41827

the four samples is 20 (S1), 135 (S2), 155 (S3), and 200 nm^2 (S4), respectively. The TEM images of these four samples are shown in Figure S1. Four CdSe NPLs samples were confirmed to have the same 4 MLs in thickness by absorption and emission at room temperature. To determine the influence of the lateral size on the low-energy peak, the PL measurement of the four samples were conducted at 30 K, as shown in Figure 3a. All other experimental conditions were kept identically, and

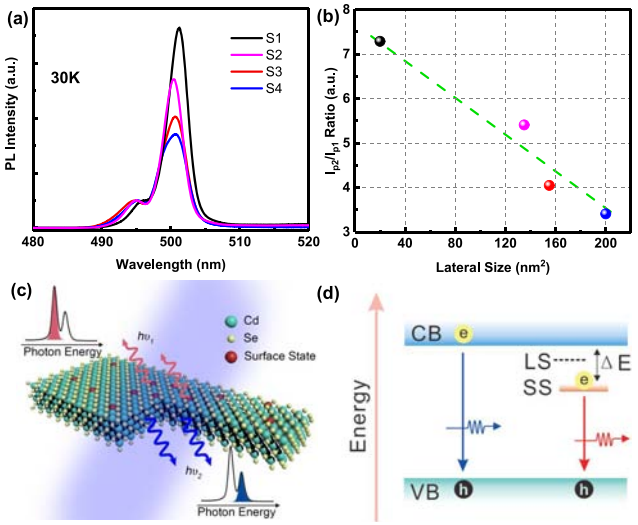

Figure 3. (a) Emission of CdSe NPLs with different lateral sizes at 30 K normalized by the intensity of the high-energy peak. (b) The ratio of the low-energy peak PL intensity (I_{p2}) to the free exciton emission intensity (I_{p1}) plotted against the lateral size. The green dash line was guided by the eye. (c) Schematic diagram of CdSe NPLs emission at low temperatures. (d) The schematic energy level of CdSe NPLs.

the PL intensities are normalized at the free exciton emission for comparison. It can be clearly observed that the intensity of the low-energy peak gradually increases with decreasing lateral size. The ratio of the low-energy peak PL intensity (I_{p1}) to the free exciton emission intensity (I_{p2}) will reflect the proportion of the surface state in the sample. Figure 3b shows the ratio of I_{p2} to I_{p1} as a function of the lateral size, where the green dash line is guided by eye. The result indicates that the low-energy emission from CdSe NPLs is closely related with their lateral size. Thus, the low-energy emission can be assigned to surface-state-related emission. Similar size-dependent surface-state-related emission has been reported in QDs.[44] In QD materials, the reduction in size influences the proportion of the surface-state-related emission, and the emission peak position has shifted due to the quantum confinement effect. However, for NPLs, the change in the lateral size only affects the surface area without changing the quantum confinement in the vertical direction. Therefore, the shift of the peak position is not observed herein, while only the proportion of the surface-state-related emission changes. It should be noted here that the defect states discussed in ref 44 is deep-level defects, which have a much lower energy than the band gap with a broad width. However, the defect states in the CdSe NPLs are considered to be shallow levels because the energy difference between the two peaks is only about 29 meV. It is also needed to mention that CdSe NPLs have a much narrow emission peak due to the precise thickness, which leads to a narrow distribution of the defect state, and therefore a narrow defect emission has been observed.

Figure 3c schematically shows the emission mechanism of 4 MLs CdSe NPLs emission at a low temperature. There are surface states near the surface of the NPLs, which come from the dangling bonds or the incomplete ligand coordination generated during the synthesis of the material.[45,46] With the decrease of the lateral size of the CdSe NPLs, the surface area to volume ratio will increase. Thus, the proportion of atoms on the surface will gradually increase, which leads to an increase of surface states. The energy-level diagram is shown in Figure 3d.

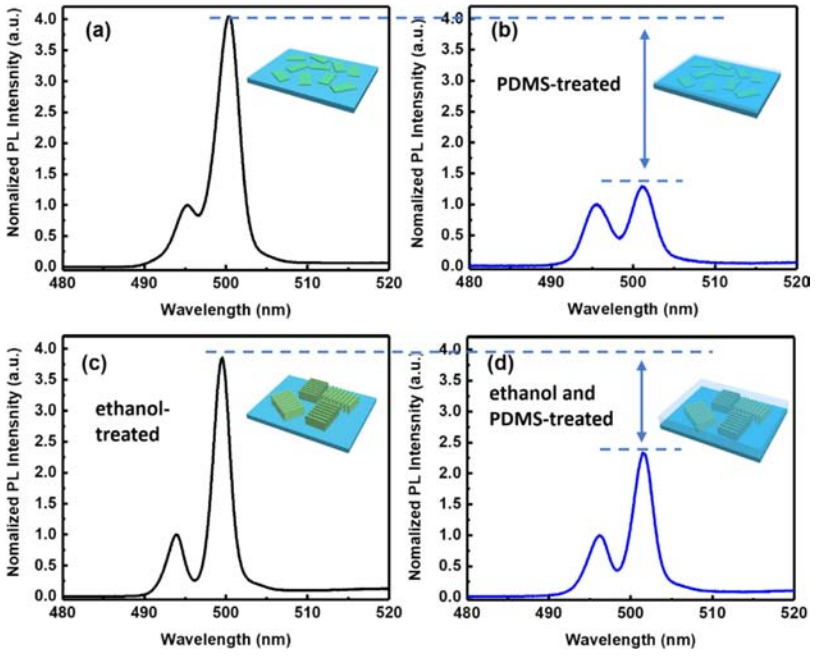

Figure 4. (a) Emission of CdSe NPLs at 40 K. (b) Emission of PDMS-covered CdSe NPLs at 40 K. (c) Emission of ethanol-treated CdSe NPLs at 40 K. (d) Emission of CdSe NPLs at 40 K, which was first treated with ethanol and then covered by PDMS.

DOI: 10.1021/acsami.9b16044
ACS Appl. Mater. Interfaces 2019, 11, 41821−41827

The surface states (SS) locate near the conduction band with energy difference ΔE around 29 meV, which is determined based on the energy difference between the surface-state-related emission and the free exciton emission at a low temperature. In addition, through fitting the temperature-dependent PL intensity, it was considered that there is a localized state (LS) with a localization depth of 10.5 meV as mentioned above. When the CdSe NPLs are excited by a laser at a low temperature, a part of the electrons are trapped by the LS and do not contribute to the emission. In addition, there are two radiative recombination pathways for the excited electrons, including free exciton emission and surface-state-related emission. The intensity of the surface-state-related emission dominating at a low temperature indicates that the surface-states-related energy level has a larger density of state. When the temperature increased, the trapped carriers thermally released from the LS induced an increase in the PL intensity. Meanwhile, the thermal energy of the electron trapped in surface state energy levels will increase and eventually escape, and the population of thermally activated nonradiative recombination centers will increase, resulting in a rapid quench of the surface-related emission.

To further confirm that the low-energy peak emission is originated from the surface states, surface treatment on the CdSe NPLs was performed. It is known that surface passivation of organic polymers on semiconductor nanomaterials can effectively reduce the number of surface defect states.[47,48] Here, poly(dimethylsiloxane) (PDMS) was selected to modify the surface of the samples because it is a common inert, nontoxic, organic polymer material with good optical transparency. The sample was prepared through drop-casting of the CdSe NPLs solution on the quartz plate. Most of the CdSe NPLs will eventually lie flat on the substrate due to the planar shape, as schematically shown in the inset of Figure 4a. Then the surface of the sample was covered with PDMS and heated for curing, as shown in the inset of Figure 4b. The low-temperature PL measurement of the untreated and the PDMS-treated sample was conducted at 40 K and the emissions are shown in Figure 4a,b, respectively. It can be found that the intensity of the surface-related emission peak is greatly suppressed after the PDMS treatment. This result verifies the relationship between the low-energy peak and the surface state of CdSe NPLs.

Due to the special quasi-two-dimensional structure of the NPLs, only some of them will self-stack when forming a solid film. It is reported that adding alcohol to the CdSe NPLs solution can accelerate the stacking during film formation, which has been demonstrated in many papers.[36,49,50] Considering that the gap between the CdSe NPLs is very narrow after forming the stacked structure, PDMS cannot enter the small gap and effectively passivates the surface. Therefore, it can be expected that the relevant PDMS treatment on low-energy peaks should be weak. Here, a similar experiment as carried out above was performed by using the alcohol-treated CdSe NPLs solution, and the PL spectra measured at 40 K are shown in Figure 4c,d. Comparing Figure 4a.c, it can be found that the stacking of CdSe NPLs did not have much effect on the PL spectra. The stacking of the CdSe NPLs did not result in a change in the intensity ratio of the surface-states-related emission to the free exciton emission. However, when comparing Figure 4b,d, it was found that the effect of surface passivation on the stacked CdSe NPLs was attenuated as suspected. PDMS that cannot enter the gap between stacked CdSe NPLs still has some passivation effect on the peripheral surface. This result further confirms that the low-energy peak is originated from the surface-state-related emission.

CONCLUSIONS

Temperature-dependent PL measurements were carried out to study the origin of two emission peaks of CdSe NPLs at a low temperature. The high-energy peak was proven to be free exciton emission through discussion of the peak position with temperature. Continuous laser irradiation increases the number of surface states of the sample, resulting in a decrease of the free exciton emission and an increase of the surface-state-related emission. The low-temperature PL measurements of four CdSe NPLs samples with different lateral sizes demonstrate the correlation between the low-energy peak and surface area to volume ratio. The surface passivation experiment with PDMS further proves that the low-energy peak originates from the surface state of CdSe NPLs.

EXPERIMENTAL SECTION

For the synthesis of 4 ML CdSe NPLs, cadmium myristate (340 mg), a certain amount of Se, and ODE (30 mL) were added in a three-neck flask. The solution was degassed under vacuum at 95 °C around 1 h. Then, the temperature of the solution was set to 240 °C under argon flow. When the temperature reached 195 °C, a certain amount of cadmium acetate dihydrate powder was added. After 10 min growth at 240 °C, 1 mL of OA was injected and the solution was moderately cooled to room temperature. Below 120 °C, 5 mL of hexane was injected for a better dissolution of NPLs. The quantum yield of the CdSe NPLs in this investigation is about 30−40%.

The CdSe NPLs solution was drop-casted on the surface of a quartz plate to form a solid film, which will be used for the optical measurements. The PDMS (Sylgard 184 Silicon, Dow Corning) was prepared by mixing liquid silicon matrix and curing agent (mass ratio 10:1). Then, the colloidal PDMS was dropped over the film to cover the CdSe NPLs. Finally, PDMS was heated for 30 min at 60 °C for curing. The low cure temperature ensures that the CdSe NPLs will not be damaged during the heating process.

The absorption spectra were tested by the Lambda 950 UV−vis spectrophotometer (PerkinElmer). Transient absorption was measured by the ExciPro femtosecond transient absorption pump-probe spectrometer (CDP Systems Corp.). The 325 nm excitation laser was transformed through Astrella ultrafast Ti:sapphire amplifier (Coherent, 800 nm, 1 KHz, 100 fs) by an ultrafast optical parametric amplifier (Coherent OperA Solo). For the PL measurement, all of the samples were excited with a 325 nm He-Cd laser (KIMMON IK5751I-G), and the signal was detected by a Newton CCD (DU920P-BU) integrated with Shamrock spectrometer (SR-750-D1-R). For the low-temperature measurements, the sample was placed on the cold finger of a helium cryostat (CRYO Cool-G2B-LT).

ASSOCIATED CONTENT

Supporting Information

The Supporting Information is available free of charge on the ACS Publications website at DOI: 10.1021/acsami.9b16044.

TEM images of four CdSe NPLs with different lateral sizes and the size distribution statistics; TEM image of the alcohol-treated CdSe NPLs (PDF)

AUTHOR INFORMATION

Corresponding Author

*E-mail: chenr@sustech.edu.cn.

ORCID

Xiao Wei Sun: 0000-0002-2840-1880

DOI: 10.1021/acsami.9b16044
ACS Appl. Mater. Interfaces 2019, 11, 41821−41827

Rui Chen: 0000-0002-0445-7847

Author Contributions

The article was written through contributions of all authors. All authors have given approval to the final version of the article.

Notes

The authors declare no competing financial interest.

■ ACKNOWLEDGMENTS

This work is supported by the National Natural Science Foundation of China (11574130) and Shenzhen Science and Technology Innovation Commission (Projects nos. KQJSCX20170726145748464, JCYJ20180305180553701, and KQTD2015071710313656).

■ REFERENCES

(1) Murray, C. B.; Norris, D. J.; Bawendi, M. G. Synthesis and Characterization of Nearly Monodisperse CdE (E = S, Se, Te) Semiconductor Nanocrystallites. *J. Am. Chem. Soc.* **1993**, *115*, 8706−8715.

(2) Mashford, B. S.; Stevenson, M.; Popovic, Z.; Hamilton, C.; Zhou, Z.; Breen, C.; Steckel, J.; Bulovic, V.; Bawendi, M.; Sullivan, S.; Kazlas, P. High-Efficiency Quantum-Dot Light-Emitting Devices with Enhanced Charge Injection. *Nat. Photonics* **2013**, *7*, 407−412.

(3) Dai, X.; Deng, Y.; Peng, X.; Jin, Y. Quantum-Dot Light-Emitting Diodes for Large-Area Displays: Towards the Dawn of Commercialization. *Adv. Mater.* **2017**, *29*, No. 1607022.

(4) Supran, G. J.; Shirasaki, Y.; Song, K. W.; Caruge, J.-M.; Kazlas, P. T.; Coe-Sullivan, S.; Andrew, T. L.; Bawendi, M. G.; Bulović, V. QLEDs for Displays and Solid-State Lighting. *MRS Bull.* **2013**, *38*, 703−711.

(5) Michalet, X. Quantum Dots for Live Cells, in Vivo Imaging, and Diagnostics. *Science* **2005**, *307*, 538−544.

(6) Medintz, I. L.; Uyeda, H. T.; Goldman, E. R.; Mattoussi, H. Quantum Dot Bioconjugates for Imaging, Labelling and Sensing. *Nat. Mater.* **2005**, *4*, 435−446.

(7) Klimov, V. I.; Mikhailovsky, A. A.; Xu, S.; Malko, A.; Hollingsworth, J. A.; Leatherdale, C. A.; Eisler, H. J.; Bawendi, M. G. Optical Gain and Stimulated Emission in Nanocrystal Quantum Dots. *Science* **2000**, *290*, 314−317.

(8) Wang, Y.; Li, X.; Song, J.; Xiao, L.; Zeng, H.; Sun, H. All-Inorganic Colloidal Perovskite Quantum Dots: A New Class of Lasing Materials with Favorable Characteristics. *Adv. Mater.* **2015**, *27*, 7101−7108.

(9) Dang, C.; Lee, J.; Breen, C.; Steckel, J. S.; Coe-Sullivan, S.; Nurmikko, A. Red, Green and Blue Lasing Enabled by Single-Exciton Gain in Colloidal Quantum Dot Films. *Nat. Nanotechnol.* **2012**, *7*, 335−339.

(10) Rainò, G.; Stoferle, T.; Moreels, I.; Gomes, R.; Kamal, J. S.; Hens, Z.; Mahrt, R. F. Probing the Wave Function Delocalization in CdSe/CdS Dot-in-Rod Nanocrystals by Time- and Temperature-Resolved Spectroscopy. *ACS Nano* **2011**, *5*, 4031−4036.

(11) Smith, E. R.; Luther, J. M.; Johnson, J. C. Ultrafast Electronic Delocalization in CdSe/CdS Quantum Rod Heterostructures. *Nano Lett.* **2011**, *11*, 4923−4931.

(12) Jia, G.; Xu, S.; Wang, A. Emerging Strategies for the Synthesis of Monodisperse Colloidal Semiconductor Quantum Rods. *J. Mater. Chem. C* **2015**, *3*, 8284−8293.

(13) Manna, L.; Milliron, D. J.; Meisel, A.; Scher, E. C.; Alivisatos, A. P. Controlled Growth of Tetrapod-Branched Inorganic Nanocrystals. *Nat. Mater.* **2003**, *2*, 382−385.

(14) Talapin, D. V.; Nelson, J. H.; Shevchenko, E. V.; Aloni, S.; Sadtler, B.; Alivisatos, A. P. Seeded Growth of Highly Luminescent CdSe/CdS Nanoheterostructures with Rod and Tetrapod Morphologies. *Nano Lett.* **2007**, *7*, 2951−2959.

(15) Lutich, A. A.; Mauser, C.; Da Como, E.; Huang, J.; Vaneski, A.; Talapin, D. V.; Rogach, A. L.; Feldmann, J. Multiexcitonic Dual Emission in CdSe/CdS Tetrapods and Nanorods. *Nano Lett.* **2010**, *10*, 4646−4650.

(16) Ithurria, S.; Dubertret, B. Quasi 2D Colloidal CdSe Platelets with Thicknesses Controlled at the Atomic Level. *J. Am. Chem. Soc.* **2008**, *130*, 16504−16505.

(17) Ithurria, S.; Bousquet, G.; Dubertret, B. Continuous Transition from 3D to 1D Confinement Observed During the Formation of CdSe Nanoplatelets. *J. Am. Chem. Soc.* **2011**, *133*, 3070−3077.

(18) Ithurria, S.; Tessier, M. D.; Mahler, B.; Lobo, R. P.; Dubertret, B.; Efros, A. L. Colloidal Nanoplatelets with Two-Dimensional Electronic Structure. *Nat. Mater.* **2011**, *10*, 936−941.

(19) Son, J. S.; Yu, J. H.; Kwon, S. G.; Lee, J.; Joo, J.; Hyeon, T. Colloidal Synthesis of Ultrathin Two-Dimensional Semiconductor Nanocrystals. *Adv. Mater.* **2011**, *23*, 3214−3219.

(20) Ithurria, S.; Talapin, D. V. Colloidal Atomic Layer Deposition (c-ALD) Using Self-Limiting Reactions at Nanocrystal Surface Coupled to Phase Transfer between Polar and Nonpolar Media. *J. Am. Chem. Soc.* **2012**, *134*, 18585−18590.

(21) Tessier, M. D.; Mahler, B.; Nadal, B.; Heuclin, H.; Pedetti, S.; Dubertret, B. Spectroscopy of Colloidal Semiconductor Core/Shell Nanoplatelets with High Quantum Yield. *Nano Lett.* **2013**, *13*, 3321−3328.

(22) Pedetti, S.; Ithurria, S.; Heuclin, H.; Patriarche, G.; Dubertret, B. Type-II CdSe/CdTe Core/Crown Semiconductor Nanoplatelets. *J. Am. Chem. Soc.* **2014**, *136*, 16430−16438.

(23) Lhuillier, E.; Pedetti, S.; Ithurria, S.; Nadal, B.; Heuclin, H.; Dubertret, B. Two-Dimensional Colloidal Metal Chalcogenides Semiconductors: Synthesis, Spectroscopy, and Applications. *Acc. Chem. Res.* **2015**, *48*, 22−30.

(24) Naskar, S.; Schlosser, A.; Miethe, J. F.; Steinbach, F.; Feldhoff, A.; Bigall, N. C. Site-Selective Noble Metal Growth on CdSe Nanoplatelets. *Chem. Mater.* **2015**, *27*, 3159−3166.

(25) Olutas, M.; Guzelturk, B.; Kelestemur, Y.; Yeltik, A.; Delikanli, S.; Demir, H. V. Lateral Size-Dependent Spontaneous and Stimulated Emission Properties in Colloidal CdSe Nanoplatelets. *ACS Nano* **2015**, *9*, 5041−5050.

(26) Guzelturk, B.; Kelestemur, Y.; Olutas, M.; Delikanli, S.; Demir, H. V. Amplified Spontaneous Emission and Lasing in Colloidal Nanoplatelets. *ACS Nano* **2014**, *8*, 6599−6605.

(27) She, C. X.; Fedin, I.; Dolzhnikov, D. S.; Dahlberg, P. D.; Engel, G. S.; Schaller, R. D.; Talapin, D. V. Red, Yellow, Green, and Blue Amplified Spontaneous Emission and Lasing Using Colloidal CdSe Nanoplatelets. *ACS Nano* **2015**, *9*, 9475−9485.

(28) Li, Q.; Xu, Z.; McBride, J. R.; Lian, T. Low Threshold Multiexciton Optical Gain in Colloidal CdSe/CdTe Core/Crown Type-II Nanoplatelet Heterostructures. *ACS Nano* **2017**, *11*, 2545−2553.

(29) Guzelturk, B.; Pelton, M.; Olutas, M.; Demir, H. V. Giant Modal Gain Coefficients in Colloidal II-III Nanoplatelets. *Nano Lett.* **2019**, *19*, 277−282.

(30) Chen, Z. Y.; Nadal, B.; Mahler, B.; Aubin, H.; Dubertret, B. Quasi-2D Colloidal Semiconductor Nanoplatelets for Narrow Electroluminescence. *Adv. Funct. Mater.* **2014**, *24*, 295−302.

(31) Cunningham, P. D.; Souza, J. B., Jr; Fedin, I.; She, C.; Lee, B.; Talapin, D. V. Assessment of Anisotropic Semiconductor Nanorod and Nanoplatelet Heterostructures with Polarized Emission for Liquid Crystal Display Technology. *ACS Nano* **2016**, *10*, 5769−5781.

(32) Giovanella, U.; Pasini, M.; Lorenzon, M.; Galeotti, F.; Lucchi, C.; Meinardi, F.; Luzzati, S.; Dubertret, B.; Brovelli, S. Efficient Solution-Processed Nanoplatelet-Based Light-Emitting Diodes with High Operational Stability in Air. *Nano Lett.* **2018**, *18*, 3441−3448.

(33) Tessier, M. D.; Biadala, L.; Bouet, C.; Ithurria, S.; Abecassis, B.; Dubertret, B. Phonon Line Emission Revealed by Self-Assembly of Colloidal Nanoplatelets. *ACS Nano* **2013**, *7*, 3332−3340.

(34) Biadala, L.; Liu, F.; Tessier, M. D.; Yakovlev, D. R.; Dubertret, B.; Bayer, M. Recombination Dynamics of Band Edge Excitons in Quasi-Two-Dimensional CdSe Nanoplatelets. *Nano Lett.* **2014**, *14*, 1134−1139.

DOI: 10.1021/acsami.9b16044
ACS Appl. Mater. Interfaces 2019, 11, 41821−41827

(35) Achtstein, A. W.; Scott, R.; Kickhofel, S.; Jagsch, S. T.; Christodoulou, S.; Bertrand, G. H. V.; Prudnikau, A. V.; Antanovich, A.; Artemyev, M.; Moreels, I.; Schliwa, A.; Woggon, U. P-State Luminescence in Cdse Nanoplatelets: Role of Lateral Confinement and a Longitudinal Optical Phonon Bottleneck. *Phys. Rev. Lett.* **2016**, *116*, No. 116802.
(36) Diroll, B. T.; Cho, W.; Coropceanu, I.; Harvey, S. M.; Brumberg, A.; Holtgrewe, N.; Crooker, S. A.; Wasielewski, M. R.; Prakapenka, V. B.; Talapin, D. V.; Schaller, R. D. Semiconductor Nanoplatelet Excimers. *Nano Lett.* **2018**, *18*, 6948−6953.
(37) Shornikova, E. V.; Biadala, L.; Yakovelv, D. R.; Sapega, V. F.; Kusrayev, Y. G.; Mitioglu, A. A.; Ballottin, M. V.; Christianen, P. C. M.; Velykh, V. V.; Kochiev, M. V.; Sibeldin, N. N.; Golovatenko, A. A.; Rodina, A. V.; Gippius, N. A.; Kuntzmann, A.; Jiang, Y.; Nasilowski, M.; Dubertret, B.; Bayer, M. Addressing the Exciton Fine Structure in Colloidal Nanocrystals: The Case of Cdse Nanoplatelets. *Nanoscale* **2018**, *10*, 646−656.
(38) O'Donnell, K. P.; Chen, X. Temperature Dependence of Semiconductor Band Gaps. *Appl. Phys. Lett.* **1991**, *58*, 2924−2926.
(39) Li, Q.; Lian, T. Area- and Thickness-Dependent Biexciton Auger Recombination in Colloidal CdSe Nanoplatelets: Breaking the "Universal Volume Scaling Law". *Nano Lett.* **2017**, *17*, 3152−3158.
(40) Narayanaswamy, A.; Feiner, L. F.; Meijerink, A.; van der Zaag, P. J. The Effect of Temperature and Dot Size on the Spectral Properties of Colloidal InP/ZnS Core-Shell Quantum Dots. *ACS Nano* **2009**, *3*, 2539−2546.
(41) Al Salman, A.; Tortschanoff, A.; Mohamed, M. B.; Tonti, D.; van Mourik, F.; Chergui, M. Temperature Effects on the Spectral Properties of Colloidal CdSe Nanodots, Nanorods, and Tetrapods. *Appl. Phys. Lett.* **2007**, *90*, No. 093104.
(42) Vaxenburg, R.; Rodina, A.; Lifshitz, E.; L. E, A. Biexciton Auger Recombination in CdSe/CdS Core/Shell Semiconductor Nanocrystals. *Nano Lett.* **2016**, *16*, 2503−2511.
(43) Tessier, M. D.; Spinicelli, P.; Dupont, D.; Patriarche, G.; Ithurria, S.; Dubertret, B. Efficient Exciton Concentrators Built from Colloidal Core/Crown CdSe/CdS Semiconductor Nanoplatelets. *Nano Lett.* **2014**, *14*, 207−213.
(44) Veamatahau, A.; Jiang, B.; Seifert, T.; Makuta, S.; Latham, K.; Kanehara, M.; Teranishi, T.; Tachibana, Y. Origin of Surface Trap States in CdS Quantum Dots: Relationship between Size Dependent Photoluminescence and Sulfur Vacancy Trap States. *Phys. Chem. Chem. Phys.* **2015**, *17*, 2850−2858.
(45) Hines, D. A.; Kamat, P. V. Recent Advances in Quantum Dot Surface Chemistry. *ACS Appl. Mater. Interfaces* **2014**, *6*, 3041−3057.
(46) Yang, J.; Deng, D. W.; Yu, J. S. Transfer from Trap Emission to Band-Edge One in Water-Soluble CdS Nanocrystals. *J. Colloid Interface Sci.* **2013**, *394*, 55−62.
(47) Liu, K. W.; Chen, R.; Xing, G. Z.; Wu, T.; Sun, H. D. Photoluminescence Characteristics of High Quality ZnO Nanowires and Its Enhancement by Polymer Covering. *Appl. Phys. Lett.* **2010**, *96*, No. 023111.
(48) Karan, S.; Majumder, M.; Mallik, B. Controlled Surface Trap State Photoluminescence from CdS QDs Impregnated in Poly-(Methyl Methacrylate). *Photochem. Photobiol. Sci.* **2012**, *11*, 1220−1232.
(49) Guzelturk, B.; Erdem, O.; Olutas, M.; Kelestemur, Y.; Demir, H. V. Stacking in Colloidal Nanoplatelets: Tuning Excitonic Properties. *ACS Nano* **2014**, *8*, 12524−12533.
(50) Erdem, O.; Olutas, M.; Guzelturk, B.; Kelestemur, Y.; Demir, H. V. Temperature-Dependent Emission Kinetics of Colloidal Semiconductor Nanoplatelets Strongly Modified by Stacking. *J. Phys. Chem. Lett.* **2016**, *7*, 548−554.

DOI: 10.1021/acsami.9b16044
ACS Appl. Mater. Interfaces 2019, 11, 41821−41827